Energy Conversion and Management 151 (2017) 357–367

Contents lists available at ScienceDirect

Energy Conversion and Management

journal homepage: www.elsevier.com/locate/enconman

Effective conversion of the carbohydrate-rich macroalgae (*Saccharina japonica*) into bio-oil using low-temperature supercritical methanol

Hassan Zeb[a], Asim Riaz[b], Jaehoon Kim[a,b,*]

[a] SKKU Advanced Institute of Nano Technology (SAINT), Sungkyunkwan University, 2066, Seobu-Ro, Jangan-Gu, Suwon, Gyeong Gi-Do 16419, Republic of Korea
[b] School of Mechanical Engineering, Sungkyunkwan University, 2066, Seobu-Ro, Jangan-Gu, Suwon, Gyeong Gi-Do 16419, Republic of Korea

ARTICLE INFO

Keywords:
Carbohydrate-rich macroalgae
Supercritical methanol
Liquefaction
Bio-oil
Solvent consumption

ABSTRACT

The use of supercritical methanol (scMeOH) for the liquefaction of the carbohydrate-rich macroalgae *Saccharina japonica* was investigated at low temperature (250–300 °C). At 300 °C, almost complete conversion (98.1 wt%) and a high bio-oil yield (66.0 wt%) were achieved. These values are higher than those achieved with supercritical ethanol (scEtOH, 87.8 wt% conversion, 60.5 wt% bio-oil yield) and subcritical water (subH_2O, 91.9 wt% conversion, 40.3 wt% bio-oil yield) under identical reaction conditions. The superior liquefaction in scMeOH is attributed to the beneficial physical properties of scMeOH, including its higher polarity, superior reactivity, and higher acidity. The superior reactivity of scMeOH was evident from the larger amount of esters (54.6 area%) produced in scMeOH as compared to that in scEtOH (47.2 area%), and the larger amount of methyl/methoxy-containing compounds (78.6 area%) produced in scMeOH than that of ethyl/ethoxy-containing compounds (58.2 area%) produced in scEtOH. The higher bio-oil yield combined with its higher calorific value (29.2 MJ kg^{-1}) resulted in a higher energy recovery of 135% for scMeOH as compared to those of scEtOH (118%) and subH_2O (96%). When considering the amount of alcohol consumed during the liquefactions and the production of light bio-oil fractions that evaporate during bio-oil recovery, the higher methanol consumption (5.3 wt%) than that of ethanol (2.3 wt%) leads to similar bio-oil yields (~51 wt%).

1. Introduction

Aquatic algae biomass is considered to be one of the most promising feedstocks for the production of biofuels and biochemicals, which is an increasingly important strategy for addressing current energy and environmental issues [1,2]. The use of algal biomass is extremely attractive owing to its natural abundance, global distribution, and the rapid CO_2 consumption that it exhibits during its growth, which is 10–20 times higher than that of terrestrial biomass [3,4]. Specifically, the use of multicellular macroalgae has enormous potential for integration with waste water treatment because multicellular macroalgae has the ability to grow in harsh conditions [5,6] and has a higher life-cycle yield compared to that of unicellular microalgae [7].

The thermochemical conversion of macroalgae into fuels and chemicals has received considerable attention recently owing to its shorter residence times and smaller space requirements than those of biochemical conversion, which is slow, requires large spaces for operation, and relies on the use of expensive enzymes. Furthermore, unlike biochemical approaches, a variety of biomass components can be treated simultaneously by thermochemical conversion [6]. On the other hand, as compared to biochemical conversion, the thermochemical conversion requires high-temperature reactor system and unspecific thermochemical reactions result in product mixtures comprised of many different types of chemicals.

Although fast pyrolysis is typically used for the thermochemical conversion of “dry” biomass into liquid fuels [8–10], hydrothermal liquefaction, which utilizes high-temperature water as a solvent, is considered to be a more appropriate choice for treating algal biomass because of its inherently high moisture content [11–16]. Indeed, there has recently been some progress in the large-scale production of bio-oil from algae using hydrothermal liquefaction [17]. Nonetheless, a significant problem with hydrothermal liquefaction is the inefficient separation of the liquid products after the liquefaction process. Liquid-liquid extraction using a non-polar or slightly polar solvent such as dichloromethane (DCM) [18], or ethyl acetate [19] is typically employed to recover the bio-oil product from the aqueous phase. However, many bio-oil components having medium-to-high polarities are not effectively extracted into the organic phase and remain in the aqueous phase [18–20]. This partitioning of products into the organic and aqueous phases during recovery not only lowers bio-oil yield, it also

* Corresponding author at: School of Mechanical Engineering and SKKU Advanced Institute of Nano Technology (SAINT), Sungkyunkwan University, 2066, Seobu-Ro, Jangan-Gu, Suwon, Gyeong Gi-Do 16419, Republic of Korea.
E-mail address: jaehoonkim@skku.edu (J. Kim).

http://dx.doi.org/10.1016/j.enconman.2017.08.092
Received 20 July 2017; Received in revised form 21 August 2017; Accepted 30 August 2017
Available online 11 September 2017
0196-8904/

complicates the study of liquefaction behavior. Furthermore, distillation, the technique most typically used to separate water from water-soluble oil fractions, is highly energy intensive and thus difficult to implement on a practical scale. Therefore, to improve hydrothermal liquefaction, effective ways to utilize the aqueous phase, which is rich both in organic compounds and inorganic ash, are required.

Organic solvents such as alcohols, acetone, 1,4-dioxane, and tetralin, especially in their supercritical states, have been employed in biomass liquefaction as alternatives to water [19,21–26]. The advantages of employing organic solvents such as alcohols like methanol, ethanol, and propanol instead of water include higher bio-oil yields, the higher calorific values of the bio-oils produced, and the production of homogeneous liquid products that do not require liquid-liquid extraction.

A variety of organic solvents have been assessed for the liquefaction of different algal biomass species. For example, Yuan et al. liquefied the microalgae *Spirulina* in methanol, ethanol, and 1,4-dioxane, and reported that of the three solvents, methanol provided the highest conversions at all the temperatures tested (300–380 °C) and a maximum conversion of 82% at 380 °C [22]. They also reported that the bio-oil yield was higher using ethanol at 340 °C (55.6 wt%) as compared to that using methanol, but the yield using methanol exceeded than that using ethanol when the temperature was raised to 380 °C (ethanol yield: 60.6 wt%, methanol yield: 62.9 wt%). Furthermore, Duan et al. assessed ten different organic solvents (i.e., ethylene glycol, methanol, ethanol, n-propanol, isopropanol, acetone, ethyl acetate, 1,4-dioxane, tetralin, and benzene) and water in the liquefaction of the microalgae *Chlorella pyrenoidosa* at 350 °C and a solvent-to-biomass ratio of 4:2.5 for 60 min [23]. They reported that ethanol was the most effective liquefaction solvent, and that the highest bio-oil yield was 64.6 wt% and the lowest solid residue yield was 11.9 wt% using an ethanol-to-biomass ratio of 12:2.5 at 350 °C for 60 min. Similarly, in a study on the liquefaction of the macroalgae *Enteromorpha prolifera* performed by Zhou et al., methanol afforded a maximum bio-oil yield of 44 wt% at 280 °C and ethanol afforded a maximum bio-oil yield of 50 wt% at 300 °C. Further increase in temperature in each case decreased the bio-oil yield [27].

In a previous study, we found that the use of supercritical ethanol (scEtOH) in the liquefaction of the carbohydrate-rich macroalgae *Saccharina japonica* at 350 °C and 29.8 MPa for 45 min resulted in high conversion (~90%) but only a moderate bio-oil yield (58.4 wt%) [28]. As the reaction temperature was increased to 400 °C, the conversion marginally increased (~94%), but the bio-oil yield increased to an exceptional 79.2 wt%. This indicated that the increase in bio-oil yield was not primarily due to the increase in biomass conversion, but because of the use of scEtOH as a reaction medium. The amount of ethanol consumed during the liquefaction at 400 °C was 18 wt%, much higher than that at 350 °C (6 wt%), indicating the more active participation of ethanol in the reaction at higher temperature. Considering the amount of ethanol consumed, the bio-oil yields were estimated to be 53.9 wt% at 400 °C and 40.0 wt% at 350 °C. Even though almost complete conversion of the carbohydrate-rich macroalgae was obtained in scEtOH at high temperature, the high consumption of ethanol, which is an expensive solvent, should be addressed carefully. In addition, because ethanol can be directly used as a transportation fuel, its high consumption during the macroalgae liquefaction makes the process less attractive in a practical-scale production of bio-oil as compared to those using water or other cheap organic solvents.

Herein, to address the problems outlined above, supercritical methanol (scMeOH) is employed as a reaction medium for the liquefaction of the macroalgae *Saccharina japonica*. We demonstrate that, at the low reaction temperature of 300 °C, almost complete conversion of the macroalgae and the high bio-oil yield of 66.0 wt% can be achieved in scMeOH. These values are much higher than those achieved with scEtOH at 300 °C (conversion: 88.0%, bio-oil yield: 60.5 wt%). In fact, the yields and conversion values obtained with scMeOH at 300 °C without the use of a catalyst are unprecedented for macroalgae liquefaction. In addition, the bio-oil produced in scMeOH exhibits a higher heating value (HHV) of 29.2 MJ kg^{-1}, which is higher than that of the bio-oil produced in scEtOH (27.8 MJ kg^{-1}). To gain insight into the liquefaction behavior of *Saccharina japonica* in scMeOH, gas chromatography coupled with time-of-flight mass spectrometry (GC-TOF/MS) was used to analyze the liquid product collected immediately after the reaction, and the analysis results are compared with those for the dried bio-oil collected after product separation. The results of scMeOH liquefaction are compared with those of scEtOH and subcritical water (subH_2O) liquefaction. The consumption of the alcohol solvents during the liquefactions and the energy recoveries are also discussed.

2. Experimental

2.1. Materials

The macroalgae *Saccharina japonica*, which is a type of kelp, was used in this study and was purchased from a local market in South Korea. The macroalgae was thoroughly washed to remove any salts present on its surface and then dried overnight in a drying oven at 105 °C. The dried macroalgae was crushed using a model IKA A11 basic analytical mill and sieved to 600–1000 μm. Because the chemical composition of the macroalgae is highly affected by seasonal variations, one batch of the feedstock was used for all the experiments in this study. Chemical composition, ultimate analysis, and inorganic content analysis results for the raw macroalgae are presented in Table 1. HPLC-grade methanol, ethanol, acetone, and DCM were purchased from Sigma-Aldrich Co. (USA). High-purity nitrogen (99.99%), helium (99.99%), hydrogen (99.99%), and air (99.99%), used for purging the reactor and in the gas chromatography experiments, were purchased from JC Gas Co. (South Korea).

2.2. Liquefaction procedure

A schematic diagram of the liquefaction and product separation protocol is shown in Fig. S2. The details of the liquefaction and product separation are described elsewhere [32]. Briefly, after adding the prerequisite amounts of macroalgae and solvent into a custom-built 140-mL SUS 316 reactor, the reactor was purged three times with nitrogen to remove the oxygen in the liquid and reactor head using a purge line dipped into the liquid. The reactor was then pressurized to 1 MPa with nitrogen. The amount of solvent (65 g) and macroalgae (6.5 g dry basis) were fixed for all the reactions. The reactor was heated to the target temperature at 15 °C min^{-1}. After the appropriate reaction time, the reactor was quenched to 100 °C in less than 5 min using cold water. After the reactor had cooled to room temperature, the gas produced during the liquefaction was passed through a wet gas meter (W-NK-2 type, Shinagawa Co., Japan) to measure its volume (the volume of 1 MPa of initially pressurized nitrogen was subtracted from the total volume), and then it was collected in a 0.5 L Tedlar® bag for compositional analysis (Step 1, Fig. S2). A small fraction of the liquid product in the reactor (~3 mL) was taken for Karl Fischer titration, chemical composition analysis via GC-TOF/MS, and for solvent quantification using GC coupled with flame ionization detection (FID) (Step 2). The solid and liquid products were poured into a beaker, weighed, and the amount of light fractions was calculated by mass balance (explained in detail in Section 3.4.3) (Step 3). The reactor was then further rinsed with acetone to collect the residual liquid and solid products. The residual solid products were separated from the liquid products using filtration (Step 4). The filter cake was dried in a drying oven at 80 °C for 24 h in order to estimate the amount of solid residue and calculate conversion (Step 5). The filtrate was evaporated using a rotary evaporator at 60 °C and 0.08 MPa for 30 min to estimate the bio-oil yield (Step 6). A control experiment was performed under identical separation conditions to ascertain that neither the liquefaction solvent

Table 1
Ultimate analysis, chemical composition analysis, and inorganic content of the raw macroalgae used in this study.

Ultimate analysis[a]						
C	H	N	S	O	H/C	O/C	HHV (MJ kg^{-1})
36.2 ± 1.3	5.0 ± 0.6	1.8 ± 0.3	0.8 ± 0.1	46.3 ± 1.6	1.66 ± 0.2	0.95 ± 0.1	14.3 ± 0.8

Chemical composition analysis (wt%)					
Carbohydrates[b]	Proteins[c]	Lipids[d]	Lignin[e]	Moisture[f]	Ash[g]
51.0 ± 1.5	14.5 ± 1.6	6.3 ± 1.2	5.6 ± 1.0	8 ± 1.0	14.7

Inorganics (ppm)[h]															
K	Ca	Na	S	Cl	P	Mg	Br	Ni	Sr	Si	Ti	Fe	Ru	Cu	Znn
119,420	106,540	84,610	59,158	24,271	8740	6007	2100	1360	978	634	598	376	211	126	98

[a] Dry, ash-free basis.
[b] By difference.
[c] Calculated by multiplying the nitrogen content by 6.25 (Kjeldahl method [29]).
[d] Measured using solvent extraction with a dichloromethane and methanol mixture (2:1 wt ratio) [30].
[e] Measured by the Klason method [31].
[f] Measured by placing the raw macroalgae sample in a drying oven at 105 °C until a constant weight was obtained.
[g] Determined using TGA (Fig. S1).
[h] Dry basis.

(methanol or ethanol) nor the rinsing solvent (acetone) remained after rotary evaporation. Two or three replicates were performed for each experiment, and the average results are reported with a standard deviation of ± 4 wt%.

A schematic of the liquefaction and separation protocol for water-based liquefaction is shown in Fig. S3. First, the product mixture from the reactor was collected using DCM as a rinsing solvent. The reaction products mixed with DCM were then filtered using DCM and water as the rinsing solvents, and the filtrate was phase-separated in a separating funnel. The aqueous phase in the separating funnel was recovered and dried until constant weight in a drying oven at 80 °C to obtain the water-soluble oil (WSO). After drying, the recovered fraction was in solid form owing to the presence of a high amount of inorganic ash (~45 wt%). The WSO fraction was determined after the combustion of the recovered solid using thermogravimetric analysis (TGA) under flowing air (Fig. S4). The filter cake was washed further with acetone and then dried in a drying oven at 80 °C for 24 h. The recovered solid residue was designated as SR-I (~34 wt% of the total solid residue). After DCM rinsing, some mixture of bio-oil and solid residue remained on the surfaces of the reactor wall and stirrer. These residues were recovered using acetone washing and filtered using acetone as the rinsing solvent. It is observed that acetone worked better as a rinsing solvent than DCM, but DCM was initially used to induce facile liquid-liquid phase separation and recovery of bio-oil. The filter cake was dried in a vacuum oven at 80 °C for 24 h. The recovered solid residue was designated as SR-II (~66 wt% of the total solid residue). Total solid residue yield was calculated by adding SR-I and SR-II. The DCM phase recovered from the separating funnel and the acetone phase were mixed together. A small fraction of the liquid product in the DCM/acetone phase (~3 mL) was taken for GC-TOF/MS analysis. The dried bio-oil was then recovered by removing the solvents using rotary evaporator at 60 °C and 0.08 MPa for 30 min.

The yields of bio-oil, WSO, and gas were calculated using Eq. (1), the yield of coke was calculated using Eq. (2), and the conversion was calculated using Eq. (3).

$$\text{Yield of bio-oil,WSO or gas (wt\%)} = \frac{\text{Mass of ash free bio-oil,WSO or gas}}{\text{Mass of dry ash free macroalgae}} \times 100 \quad (1)$$

$$\text{Yield of coke (wt\%)} = \frac{\text{Mass of solid residue} - \text{Mass of inorganics in the solid residue}}{\text{Mass of dry ash free macroalgae}} \times 100 \quad (2)$$

$$\text{Conversion (wt\%)} = \frac{\text{Mass of dry ash free macroalgae} - \text{Mass of organics in solid residue}}{\text{Mass of dry ash free macroalgae}} \times 100 \quad (3)$$

The HHV of the produced bio-oil was calculated according to the DIN 51900 standard:

$$\text{HHV (MJ kg}^{-1}) = (34\,C + 124.3\,H + 6.3\,N + 19.3S - 9.8O)/100 \quad (4)$$

where C, H, N, S, and O are the weight percentages of carbon, hydrogen, nitrogen, sulfur, and oxygen, respectively, and were obtained using elemental analysis.

Energy analysis of the two liquefaction processes was performed based on energy recovery, which is the ratio of energy obtained from the bio-oil to the energy present in the raw feedstock and is calculated using Eq. (5).

$$ER = \frac{(HHV_{oil} \times m_{oil})}{(HHV_{raw} \times m_{raw})} \times 100 \quad (5)$$

2.3. Product characterization

The total inorganic ash content was measured using TGA (Q50, TA Instruments) over a temperature range of 30–800 °C at a heating rate of 10 °C min^{-1} and an air flow rate of 40 mL min^{-1}. The carbon, hydrogen, nitrogen, and sulfur contents in the raw macroalgae and the produced bio-oil were quantified using a model Vario EL cube elemental analyzer equipped with a thermal conductivity detector (TCD), manufactured by Elementar Analysensysteme GmbH (Germany), and the oxygen content was measured using the TCD detector in O-mode. The organic composition of the liquid product collected as soon as the reactor was opened was analyzed using an Agilent Technologies 7890A GC with a Pegasus high-throughput TOF/MS detector (Leco Corporation, USA). The GC was equipped with a 7683B series auto-injector (Agilent Technologies) and an Rxi-5ms medium polarity

column (30 m × 0.25 mm × 0.25 μm). A 1 μL of bio-oil solution in acetone was injected into the column using a split ratio of 50:1. The injector temperature was set at 260 °C. The temperature was programmed to start at 40 °C for 3 min and then increase to 300 °C at 5 °C min^{-1} and maintained at 300 °C for 5 min. The compounds were identified using the National Institute of Standards and Technology MS search 2.0. The inorganic compositions of the metallic species in the macroalgae samples were analyzed using an S4 Bruker X-ray fluorescence (XRF) spectrometer. Water content was determined by the Karl Fischer titration method using a Metrohm 877 Titrino plus (Switzerland). Details of the above mentioned characterization tools have been provided elsewhere [32]. The amount of alcohol remaining after the liquefaction reaction was quantified using a model 6890A GC-FID (Agilent Technologies) and an Rxi®-5Sil MS (30 m × 0.25 mm × 0.25 μm) column. The GC was operated with ultra-high purity helium as the carrier gas at a constant flow rate of 1.0 mL min^{-1}. The GC inlet temperature and the detector temperature were both set at 250 °C, and a split ratio of 1:10 was used. The oven temperature was held at 40 °C for 2 min before it was raised to 250 °C at 20 °C min^{-1}, and it was held there for 3 min. The gaseous products, comprising H_2, CO_2, CO, CH_4, C_2H_6, C_2H_4, and C_3–C_5 compounds, were quantified using refinery gas analyser gas chromatography (RGA-GC). Nitrogen, which was used to pressurize the reactor prior to temperature ramping, was not included in the composition analysis. The GC instrument (Clarus 580 GC-Model Arnel 1115PPC refinery gas analyzer; Perkin Elmer, USA) was equipped with both a TCD and an FID. The detailed specifications of the RGA-GC system are provided elsewhere [33].

3. Results and discussion

3.1. Effects of reaction temperature

The effects of reaction temperature on bio-oil yield and macroalgae conversion were investigated, as shown in Fig. 1a. Even at the low reaction temperature of 250 °C, the yield of bio-oil is as high as 53.1 wt%. However, the 74.6% conversion obtained at 250 °C is still low, indicating the possibility of enhancing conversion and bio-oil yield by using higher reaction temperatures. As the reaction temperature increases to 275 °C, the conversion increases to 85.4% and the bio-oil yield increases to 64.1 wt%. Enhanced thermal decomposition of solid biomass was expected to occur with increasing temperature, which could decrease the coke yield from 25.7 wt% at 250 °C to 14.8 wt% at 275 °C. Further increase in temperature to 300 °C results in almost complete conversion of the macroalgae, but the bio-oil yield only marginally increases to 66.0 wt%. It is noted that the bio-oil yields at 275–300 °C are higher than those reported from most comparable previous studies concerning algae biomass in water or organic solvents with and without the use of catalyst. When measured at similar temperatures, the yields reported for these similar studies are generally in the range 20–60 wt% [24,34–36]. In fact, no previous study has achieved the complete conversion of macroalgae biomass at the low temperature of 300 °C in the absence of catalyst. The complete conversion of the solid macroalgae at the moderate temperature of 300 °C in the absence of catalysts and the high bio-oil yield constitute a significant advance for the practical-scale implementation of this strategy.

The excellent conversion and bio-oil yield observed in this study could be due to the beneficial role of scMeOH and the choice of feedstock. The role of scMeOH for enhancing the conversion of carbohydrate-rich algae will be discussed in detail in Section 3.4.1. The selection of feedstock seems to be one of the most important parameters. Previous algal biomass liquefaction studies have focused on lipid-rich and protein-rich algal strains [37–41], but the need for de-nitrogenation of the bio-oil produced from protein-rich algal species makes this feedstock less appealing as compared to lipid-rich algae. Conversely, a relatively limited number of studies have focused on carbohydrate-rich algal strains as compared to the number that have focused on lipid-rich

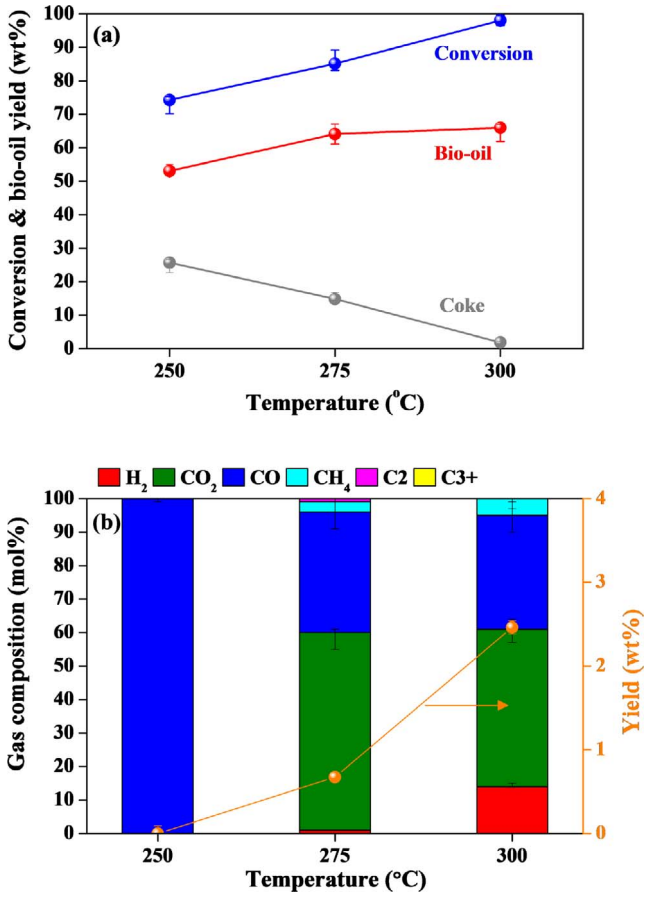

Fig. 1. Effects of reaction temperature on (a) macroalgae conversion and bio-oil yield, and on (b) yield and composition of gases produced. Reaction conditions: 250 °C (13.8 MPa), 275 °C (19.9 MPa), 300 °C (27.2 MPa), and 9.1 wt% for 30 min.

algae [18,20,27,42–47]. A significant amount of the liquid products obtained from the decomposition of carbohydrates in hydrothermal liquefaction tend to reside in the aqueous phase during liquid-liquid extraction. Therefore, the yield of bio-oil recovered from the organic phase is low (9–26 wt%) and the yield of WSO is very high (> 60 wt%) for carbohydrate-rich algae [18,42,43]. In addition, it is not easy to recover all the WSO fraction using simple distillation. Conversely, when lipid-rich algae are used, highly hydrophobic bio-oils with long-chain fatty acid components are produced, and thus the produced bio-oil prefers to stay in the organic phase. This leads to an increase in the amount of bio-oil recoverable using liquid-liquid extraction (39–52 wt %) [48].

Almost compete conversion of the organic species in the macroalgae and a low gas yield (less than 3 wt%, Fig. 1b) are achieved, but the moderate bio-oil yield suggests that some liquefied bio-oil fractions are not recovered during product separation. One of the possible reasons for this is that the light bio-oil fractions evaporate from the filtrate during the separation and washing steps.

Fig. S5 shows the GC-TOF/MS chromatograms of the light bio-oil fractions that are collected in the receiving flask (which was connected to the rotary evaporator) and in the cold trap (which was connected to the vacuum oven). The ten most abundant chemical species collected in the receiving flask (e.g., acetic acid methyl ester, methyl propionate, 4-hydroxy-4-methyl-2-pentanone, and pyrrole, 2-butanone) and the cold trap (e.g., acetic acid methyl ester, methyl propionate, 2-butenoic acid methyl ester, 2-methyl-butanal, and 1-methyl-1H-pyrrole) are listed in Tables S1 and S2, respectively. Similar chemical species are detected in the light bio-oil fractions produced at 275 and 300 °C. The light fraction produced at 300 °C shows higher peak intensities and higher total area

of the 10 most abundant compounds as compared those for the light fraction produced at 275 °C, indicating that a higher degree of decomposition occurs at higher temperature resulting in greater loss of lighter species during the solvent removal step. This may be the reason for the similar yields of bio-oil produced at 300 and 275 °C, despite the considerable increase in conversion from 85.4% at 275 °C to 98.1% at 300 °C.

Fig. 1b shows the yields and compositions of the gases produced at different reaction temperatures. A negligible amount of gas is produced at 250 °C, most of which is CO. As the temperature increases to 300 °C, the gas yield increases and the composition of the gas changes. The major gas species produced at 300 °C is CO_2 followed by CO and H_2. The presence of CO at 250 °C and that of CO_2 with increasing temperature to 300 °C indicates that decarbonylation is major pathway at 250 °C, while decarboxylation is activated at 300 °C. The compositional change at 300 °C also suggests the possible decomposition of methanol producing a mixture of CO_2 and synthesis gas (H_2 + CO). The methanol participation in the liquefaction reaction will be discussed in detail in Section 3.4.3. Control experiments with 65 g of methanol and no macroalgae were conducted at 250–300 °C for 30 min to assess the self-decomposition of methanol under the liquefaction conditions. However, no gas formation is observed, indicating that the active intermediate species generated from the decomposition of macroalgae activate methanol decomposition, resulting in an increased gas yield. In order to check possibility of enhanced methanol decomposition in the presence of ash in the macroalgae, another control experiment with 65 g of methanol and 1 g of ash (which was produced by the calcination of macroalgae at 800 °C for 1 h under air flow condition) was conducted. As shown in Figs. S6 and S7, only a negligible amount of CO_2 (less than 0.002 wt%) was produced from methanol in the presence of ash. This suggests that the presence of ash did not affect significantly the methanol decomposition to gases under the reaction conditions examined in this study. However, as shown in Fig. S8, the liquid phase analysis using GC-TOF/MS indicates that in the presence of ash, 2,5-dimethlycyclopentanone and 2-methyl-1-penten-3-one, which were not observed in the control experiment without ash, were observed. Therefore, the decomposed product of macroalgae constituents could contribute to form gases observed in Fig. 1b. However, in the system comprising a mixture of biomass and solvent, identifying which gas species are generated by which component is extremely difficult.

3.2. Effects of residence time

The effects of residence time on the conversion and bio-oil yield at a fixed temperature of 300 °C are shown in Fig. 2a. The time taken for the temperature to reach 300 °C (~20 min) and the reactor cooling time (5 min to drop below 100 °C) are not included in the residence time, although some reaction may occur during these periods. For the residence time of 0 min, heating was stopped and the reactor was quenched as soon as the reaction reached the set temperature.

An increase in residence time from 0 to 15 min enhances the conversion from 80.1 to 94.8% and the bio-oil yield from 60.5 to 66.0 wt%. When the residence time is further increased to 30 min, almost complete conversion is achieved, but the yield of bio-oil produced over 30 min is very similar to that produced over 15 min. Again, the increased production of light fractions under the extended residence time of 30 min, which subsequently evaporate from the filtrate during the solvent removal step, leads to the similar bio-oil yields. However, higher conversion is observed for the extended residence time. The GC-TOF/MS chromatograms of the light bio-oil fractions produced over 15 and 30 min are shown in Fig. S9. The most abundant chemical species collected in the receiving flask (e.g., acetic acid methyl ester, methyl propionate, 4-hydroxy-4-methyl-2- pentanone, 1-methyl-1H-pyrrole, and 2-butanone) and in the cold trap (e.g., acetic acid methyl ester, methyl propionate, 2-butenoic acid methyl ester, 2-methoxy-propanoic acid methyl ester, and 2,5-dimethyl-1H-pyrrole) are listed in Tables S3 and S4,

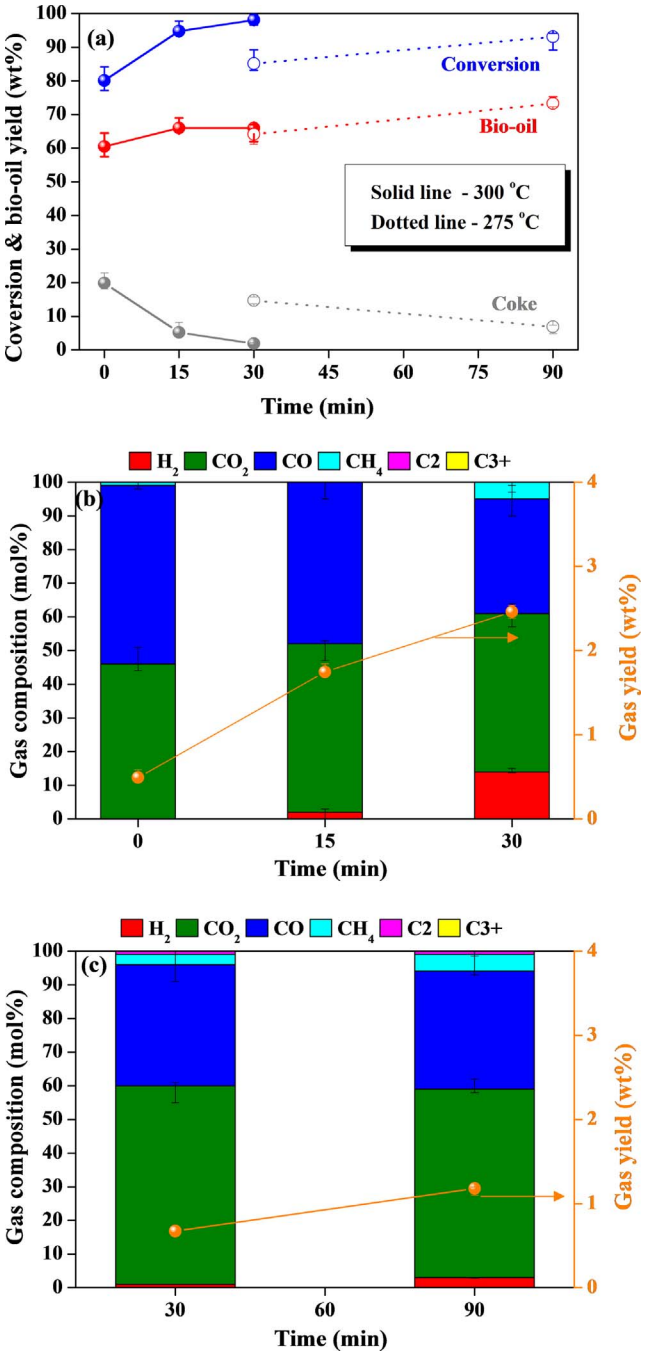

Fig. 2. Effect of residence time on (a) macroalgae conversion and bio-oil yield, (b) gas yield and its composition at 300 °C, and (c) gas yield and its composition at 275 °C. Reaction conditions: 300 °C, 0 min (26.7 MPa), 15 min (27.2 MPa), 30 min (27.2 MPa), and 9.1 wt% for 30 min; 275 °C, 30 min (19.9 MPa), 90 min (20.6 MPa).

respectively. The light fractions produced over 30 min present higher intensity peaks and total peak areas for the most abundant compounds as compared to those produced over 15 min, indicating that extended reaction time facilitates the decomposition of bio-oil.

A similar trend for residence time has been reported in previous studies, in which an increase in residence time first increased the bio-oil yield until it reached a peak level, after which further increase in residence time either decreased or did not affect the bio-oil yield [13,20,49–52]. For example, Valdez et al. studied the hydrothermal liquefaction of *Nannochloropsis* sp. and reported that the bio-oil yield reaches a maximum value of 52 wt% at 10 min, after which increasing the reaction time decreases the bio-oil yield [49]. In a typical

hydrothermal liquefaction, an extended reaction time facilitates recombination (repolymerization/condensation) of the reaction intermediates, resulting in increased char/tar yields as well as the production of gas, and thus the bio-oil yield decreases [36,53]. Conversely, when biomass liquefaction is carried out in the presence of a hydrogen donating solvent (e.g., tetraline or ethanol) the bio-oil yield does not decrease with increased residence time [19,54,55]. This is because, in the presence of hydrogen donating solvents, active intermediates are effectively quenched by hydrogen, and thus recombination reactions are suppressed [19].

To investigate the effect of reaction time at low reaction temperatures, liquefaction was conducted at 275 °C, as shown in Fig. 2a. The conversion slightly increases from 85.2 to 93.1% upon increasing the reaction time from 30 to 90 min, but the conversion at 275 °C over 90 min is lower than that at 300 °C over 30 min. This indicates that the high reaction temperature plays a crucial role in accomplishing complete conversion of the macroalgae. A rather surprising result is that the highest bio-oil yield of 72.1 wt% is achieved at 275 °C over 90 min despite the lower conversion as compared to that at 300 °C over 30 min. This indicates that the cracking reaction occurs less at the lower temperature and thus higher-molecular-weight products are produced. This heavy bio-oil fraction can remain in the evaporation flask during the solvent removal step, thus increasing the bio-oil yield. The results for the lower-temperature and longer-residence-time reaction (275 °C and 90 min) also indicate that there is a thermal energy barrier to the complete decomposition of solid macroalgae into liquid bio-oil.

The yields and compositions of gases produced under different reaction times are shown in Fig. 2b. With the increase in reaction time from 0 to 30 min, a steady increase in gas yield from 0.5 to 2.4 wt% is observed. This can be because of the increased decomposition of the reaction intermediates with increasing reaction time. The gases produced are comprised of almost equal amounts of CO and CO_2, implying that the decarbonylation and decarboxylation of reaction intermediates are the two-major gas producing phenomena during the liquefaction. When the residence time increases from 30 to 90 min at 275 °C (Fig. 2c), the yield and composition of the gas changes little. The yield of gas produced at 275 °C over 90 min is lower than that produced at 300 °C over 30 min, indicating that the decomposition reaction is more affected by an increase in temperature than an increase in residence time.

3.3. Bio-oil composition analysis

Most previous studies on biomass liquefaction have typically involved analysis of the chemical compositions of dried heavy bio-oil fractions [13,14,23,41,46,50,55–58]. Because of the absence of data for light bio-oil fractions, the full potential of bio-oil fractions produced during liquefaction reactions is not fully appreciated. This is because significant amounts of light fractions (20–25 wt% based on mass balance and depending on reaction conditions) are typically lost during the product separation process [28]. However, the separation protocol developed in this study allows analysis of the light fractions collected in the receiving flask and the cold trap during the solvent removal steps. To the best of our knowledge, neither the liquid products collected immediately at the end of liquefaction nor the light bio-oil fractions derived have been analyzed previously.

Fig. 3a shows a comparison of the GC-TOF/MS chromatogram of the liquid mixture collected as soon as the reactor was opened with that of the dried bio-oil, and Fig. 3b shows a comparison of the chromatogram of the light bio-oil fraction with that of the dried bio-oil. Detailed analyses of the individual compounds in the liquid products and their classification into oxygen- or nitrogen-containing species will be discussed in Section 3.4.4, where scMeOH liquefaction is compared with scEtOH and subH_2O liquefaction. Here, a brief comparison of the liquid product collected as soon as the reactor was opened and the dried bio-oil is presented to accentuate the importance of the product separation protocol for a deeper understanding of liquefaction behavior. Most of the light fractions are detected at retention times below 8 min, including acetic acid methyl ester (1 in Fig. 3a), lactic acid (2), methyl propionate (7), 2-methoxy-propanoic acid methyl ester (10), pyrrole (11), 2-butanone (12), 1-methyl-1H-pyrrole (13), and 2-butenoic acid methyl ester (14). The partitioning of the light fractions and dried bio-oil can be seen in Fig. 3b. The light fractions either present very small area% values or are not detected at all in the dried bio-oil. These oxygen-rich species decrease the overall HHV if they constitute part of the bio-oil, but some of them are enormously useful as value-added chemicals. For example, acetic acid methyl ester is a precursor for producing acetic acid, which is widely used as a disinfectant, as an active component of vinegar [59], and for the production of chemicals such as ethanol [60] and vinyl acetate [61]. Lactic acid, which is found in high area% in the light fractions, has a number of applications in the food and pharmaceutical industries and is a precursor for propylene glycol and the biodegradable polymer poly(lactic acid) [62]. Other C3 and C4 esters can be utilized in their acidic forms after hydrolysis as building blocks in the chemical industry and in the agricultural sector. For example, propanoic acid can be used as a preservative in the food industry without modification and its salts with alkali or alkaline earth metals can be used in agriculture as animal feeds and as food preservatives [63].

In the dried bio-oil chromatogram, the species present in higher area% appear after 8 min retention time and include 9-octadecenoic acid methyl ester (3 in Fig. 3a), 14-methyl-pentadecanoic acid methyl ester (4), pentanedioic acid dimethyl ester (5), butanedioic acid dimethyl ester (6), methyl tetradecanoate (8), and 2-methyl-propanoic acid anhydride (9). Because of their high molecular weights, these species do not evaporate and hence their relative abundance in the dried bio-oil increases upon evaporation of the lighter fractions.

3.4. Comparison of scMeOH liquefaction with scEtOH and subH_2O liquefaction

In our previous work, scEtOH-based liquefaction was employed on the same algal strain (*Saccharina japonica*) as is used in the current study and a bio-oil yield of 49.9 wt% was obtained at 300 °C [28]. However, the compositions of feedstocks used in the previous study (66.0 wt% carbohydrates, 10.6 wt% protein, and 1.6 wt% lipid) and that used in the current study (51.0 wt% carbohydrates, 14.5 wt% protein, 6.3 wt% lipid, and 5.6 wt% lignin) are different. Although the macroalgae strain was the same, different origins and seasonal variations can result in different growth conditions, and thus variations in the macroalgae constituents can occur. Therefore, the different compositions of the macroalgae necessitates rerunning the scEtOH-based liquefaction experiment at 300 °C for fair comparison. In addition, because hot water is often the first-choice solvent for algal biomass liquefaction, subH_2O-based liquefaction was also conducted at 300 °C and the results are compared with those of scMeOH-based liquefaction.

3.4.1. Yield, conversion, and gas composition

Fig. 4a shows a comparison of the conversions and product yields obtained using scMeOH, scEtOH, and subH_2O at 300 °C. The conversion rates are in the order scMeOH (98.1%) > subH_2O (91.9%) > 87.8% (scEtOH) while the bio-oil yields are in the order scMeOH (66.0 wt %) > scEtOH (60.5 wt%) > subH_2O (40.3 wt%). This indicates that the scMeOH-based liquefaction is more effective for the conversion of *Saccharina japonica*. In the case of the subH_2O-based liquefaction, an additional WSO yield of 12.9 wt% is observed, which makes the total organic yield 53.2 wt% (bio-oil + WSO). The WSO yield may be underestimated because of the severe drying conditions employed for WSO recovery, which might cause greater loss of light bio-oil fractions. This could be the reason for the lower yield of bio-oil + WSO in the case of subH_2O-based liquefaction, despite its higher conversion compared to that of scEtOH-based liquefaction.

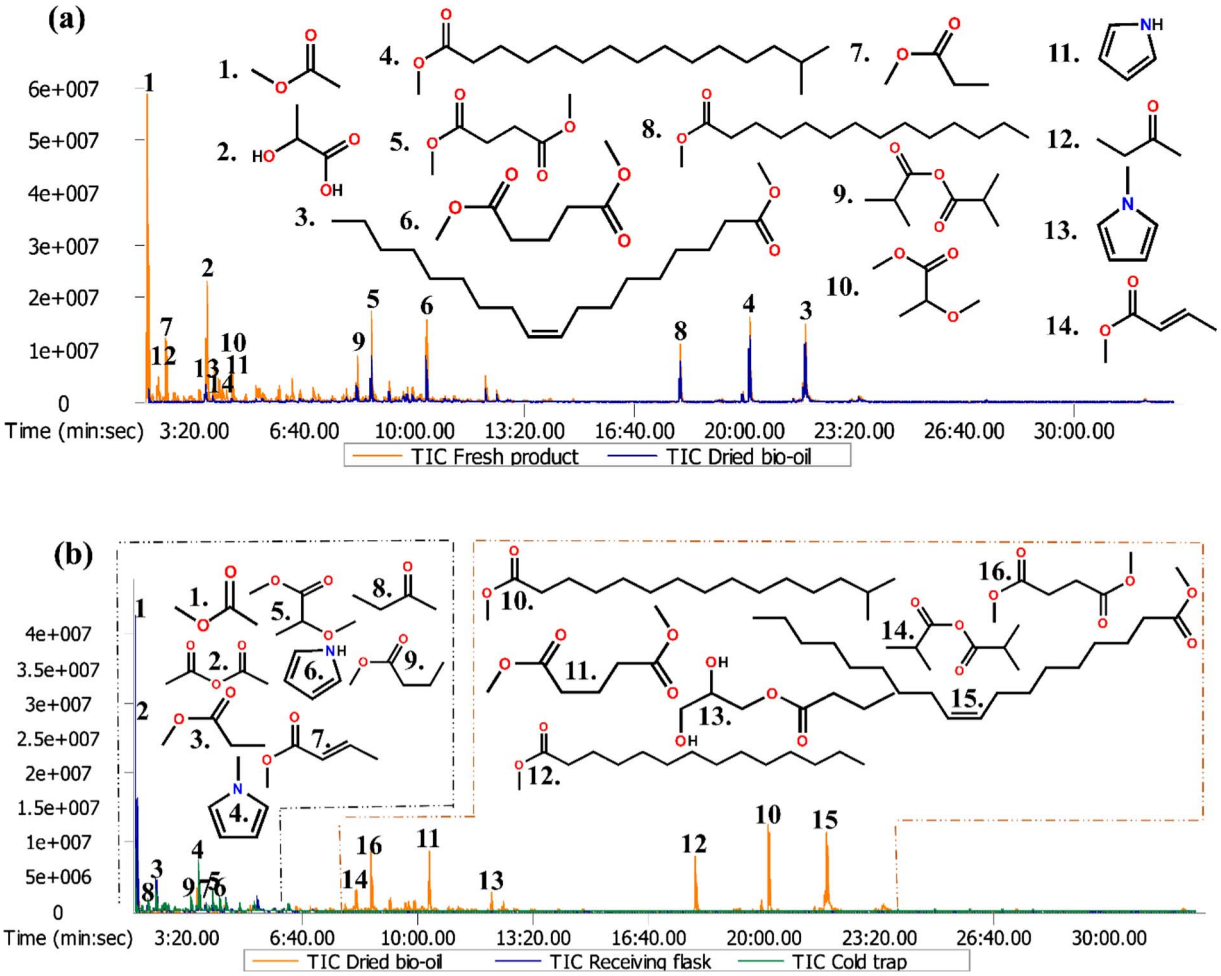

Fig. 3. Comparison of the GC-TOF/MS chromatograms for (a) the liquid mixture collected as soon as the reactor was opened (orange color) the dried bio-oil (blue color), and (b) the light bio-oil fractions that were collected in the receiving flask (blue color) and the cold trap (green color) and the dried bio-oil (orange color). Reaction conditions: 300 °C, 27.2 MPa, and 9.1 wt% for 30 min. (For interpretation of the references to colour in this figure legend, the reader is referred to the web version of this article.)

The performances of scMeOH and scEtOH in the liquefaction of algal biomass have been widely researched, and contrary results have been observed in different studies. For example, Duan et al. [23] and Zhou et al. [27] performed microalgae (*Chlorella pyrenoidosa*) and macroalgae (*Enteromorpha prolifera*) liquefactions, respectively, and concluded that higher yields are obtained with scEtOH-based liquefaction. Duan et al. reported a bio-oil yield of 75.2 wt% for scEtOH-based liquefaction and a bio-oil yield of 63.2 wt% for scMeOH-based liquefaction conducted at 350 °C [23]. Zhou et al. reported a bio-oil yield of 50 wt% (at 300 °C) and 44 wt% (at 280 °C) for scEtOH- and scMeOH-based liquefactions, respectively [27]. Singh et al. reported a higher yield of bio-oil with the use of scMeOH (59.0 wt%) compared to that with scEtOH (53.6 wt%) when the macroalgae *Ulva fasciata* was liquefied at 300 °C [42]. A number of different solvents have been investigated for biomass liquefaction, and the different effects of solvents have been explained primarily on the basis of their polarities and ability to generate active species such as hydrogen [22,27,56,58,64]. In addition to these solvent effects, the differences in the physical properties of methanol and ethanol can be correlated with the results observed in this study as follows: (a) Generally, the action of a solvent during a typical biomass liquefaction starts with its penetration into the intercellular/intracellular matrix of the biomass, which causes it to swell. This swelling results an increase in the internal surface area and a widening of the intermolecular linkages, thus weakening the macromolecular interactions and making the bulk structure more amenable to thermal decomposition and chemical reaction [22]. The penetration of solvent molecules into the biomass structure depends on the molecular size of the solvents. Because methanol is smaller than ethanol, it is more able to penetrate into biomass matrices. (b) Methanol can provide a more acidic environment as compared to that provided by ethanol [65], promoting the solvolysis of carbohydrates [66]. (c) The reaction intermediates/products derived from carbohydrates typically contain oxygen-containing medium-polarity species (e.g., furans, carboxylic acids, and ketones), which are highly reactive and are easily repolymerized to form tar/coke if their recombination is not properly suppressed. The superior reactivities of scMeOH in methylation, methoxylation, and esterification as compared to those of scEtOH allow it to more effectively quench the reactive intermediates [67,68].

The high gas yield for water-based liquefaction in high-temperature media (Fig. 4a) indicates enhanced decomposition of the reaction intermediates. Fig. 4b shows a composition of the gases produced during scMeOH-, scEtOH-, and subH_2O-based liquefactions. The major decomposition pathway in subH_2O is the decarboxylation reaction, producing CO_2 as a dominant species. This result is in good agreement with previous studies on hydrothermal liquefaction of algal biomass [11–13]. Other minor species for subH_2O-based liquefaction include CO and very small amounts of H_2. When alcohols are used as liquefaction solvents, the decomposition of the solvent as well as the macroalgae and reactions between the solvent and the macroalgae make it more difficult to elucidate accurate gas formation mechanisms. Although the major gas component is CO_2 for both alcohols, a considerable amount of CO is generated. A significant amount of H_2 is also produced using

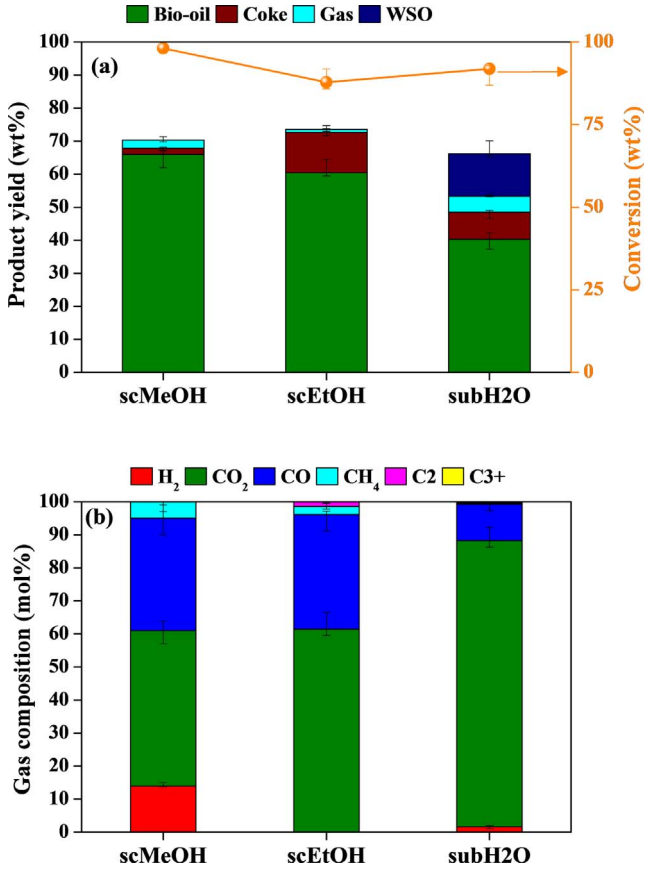

Fig. 4. Comparison of the scMeOH-, scEtOH-, and subH$_2$O-based liquefactions. (a) Macroalgae conversion, bio-oil yield, and gas yield, and (b) gas composition. Reaction conditions: 300 °C, 27.2 MPa (scMeOH), 21.9 MPa (scEtOH), 10.1 MPa (subH$_2$O), 9.1 wt % for 30 min.

scMeOH, which is thought to originate from methanol self-decomposition (which may be assisted by macroalgae components) producing a mixture of CO_2 and synthesis gas.

3.4.2. Energetics

Table 2 lists the C/H/N/S/O contents and HHV values of the bio-oils produced at different temperatures (250, 275, and 300 °C) by scMeOH-based liquefaction. Energy analysis was performed based on energy recovery (ER) values (Eq. (5)), which take into consideration both the yields and calorific values of the bio-oils. Compared to the values for the raw macroalgae (O, 46.3 wt%; C, 36.2 wt%; H, 5.0 wt%), the O content of the bio-oil produced at 250 °C is significantly lower (21.1 wt %) and both the carbon and hydrogen contents (59.4 and 7.0 wt%, respectively) are higher. There are at least two possible explanations for the removal of oxygen during the scMeOH liquefaction; (1) the removal of oxygen in the form of gaseous species (CO is observed to be the only gaseous component at 250 °C); and (2) selective partitioning of highly oxygenated species into the coke phase. Decomposed intermediates with high oxygen functionality are highly reactive and may preferentially repolymerize to form coke and/or char. The coke yield at 250 °C is as high as 25.7 wt%. Since the gas yield at 250 °C is quite low (0.06 wt%, see Fig. 1b), coke formation is thought to be the dominant mechanism for this oxygen loss. In addition, the preferable partitioning of light oxygenated species in the light fraction could be responsible for oxygen removal.

When the temperature is raised to 300 °C, the oxygen content decreases further to 17.8 wt% and a carbon-rich bio-oil (64.9 wt%) is produced. At this temperature, the gas yield is also increased to 2.5 wt% and the composition of the gas changes from CO alone to a mixture of CO_2, CO, H_2, and CH_4. This indicates that additional oxygen removal mechanisms (e.g., decarboxylation) play roles in the low oxygen content of the bio-oil. The increased oxygen removal at the higher reaction temperature (300 °C) increases the HHV from 14.3 MJ kg^{-1} for the untreated macroalgae to 29.2 MJ kg^{-1}.

The results of scMeOH liquefaction at 300 °C were compared with those of scEtOH and subH$_2$O liquefaction under identical temperature conditions, as shown in Table 2. The bio-oil produced in scMeOH retains slightly more carbon than that produced in the scEtOH-produced bio-oil while the contents of the other elements are similar for both. Consequently, the HHV of the bio-oil produced in scMeOH is slightly higher than that produced in scEtOH. A plausible mechanism for the carbon enrichment of the scMeOH bio-oil is methylation/methoxylation, which will be discussed in Section 3.4.4. Since the yield of bio-oil produced in scMeOH is higher (66.0 wt%) than that produced in scEtOH (60.5 wt%), the combination of the higher bio-oil yield and the higher HHV results in the higher ER of 135% for scMeOH liquefaction as compared to 118% for the scEtOH liquefaction.

In the case of subH$_2$O liquefaction, the bio-oil recovered from the DCM/acetone-soluble phase exhibits a much higher carbon content (74.3 wt%) and HHV value (34.1 MJ kg^{-1}) because the hydrophobic bio-oil fractions are partitioned preferentially into the DMC phase. However, despite producing high-energy-content bio-oil, the ER value of the DCM/acetone-soluble bio-oil is much lower (96%) than those from the scMeOH- and scEtOH-based liquefactions because of the low bio-oil yield. Conversely, highly oxygenated species, being polar in nature, reside in the aqueous phase, and thus the carbon content (27.8 wt%) and HHV (11.9 MJ kg^{-1}) of the WSO are much lower than those of the DCM/acetone-soluble fraction.

3.4.3. Solvent consumption

Considering the reactive nature of the supercritical alcohols used in this study, some of the solvent used for the liquefaction may participate in the reaction. Consequently, the amount of solvent consumed during liquefaction at 300 °C was investigated. The total mass of the product collected as soon as the reactor was opened consisted of unreacted solvent, bio-oil, solid residue, water produced during the reaction, and

Table 2
C, H, N, S, and O contents, HHV values, and ER values for scMeOH, scEtOH, and subH$_2$O-based liquefactions.

			C (wt%)	H (wt%)	N (wt%)	S (wt%)	O (wt%)	HHV (MJ kg^{-1})	ER (%)
Macroalgae			36.2 ± 1.3	5.0 ± 0.6	1.8 ± 0.3	0.8 ± 0.1	46.3 ± 1.6	14.3 ± 0.8[a]	
scMeOH	250 °C	Bio-oil	59.4 ± 1.2	7.0 ± 0.5	1.1 ± 0.5	2.0 ± 0.3	21.1 ± 1.4	27.3 ± 1.3	101 ± 1.8
	275 °C		62.8 ± 1.4	6.8 ± 0.7	3.1 ± 0.4	1.8 ± 0.1	17.6 ± 1.3	28.7 ± 1.1	129 ± 1.6
	300 °C		64.9 ± 1.7	6.6 ± 0.7	3.0 ± 0.4	2.2 ± 0.3	17.8 ± 1.1	29.2 ± 1.5	135 ± 2.4
scEtOH	300 °C	Bio-oil	60.3 ± 1.4	6.7 ± 0.6	2.9 ± 0.6	2.4 ± 0.1	17.4 ± 0.9	27.8 ± 1.3	118 ± 2.0
subH$_2$O	300 °C	Bio-oil	74.3 ± 1.6	7.5 ± 0.4	2.8 ± 0.6	2.7 ± 0.3	13.0 ± 1.6	34.1 ± 1.5	96 ± 2.1
		WSO	27.8 ± 1.3	4.3 ± 0.3	0.9 ± 0.2	2.4 ± 0.3	34.8 ± 2.5	11.9 ± 2.1[a]	20 ± 1.3

[a] Based on whole biomass and product including ash.

the light fractions, and was calculated using Eq. (6)

$$\text{Mass of product } (m_r) = \text{Mass of (unreacted solvent + bio-oil + solid residue + water + light fractions)} \quad (6)$$

The amount of unreacted alcohol was measured using GC-FID. The amount of water produced during the liquefaction was measured using Karl Fischer titration. The amounts of bio-oil and solid residue produced were calculated using Eqs. (1) and (2), respectively. Therefore, the amount of light fractions produced can be calculated using Eq. (6). Based on the alcohol consumption, the yields of bio-oil produced in scMeOH and scEtOH were redefined using Eq. (7) and ER was redefined using Eq. (8). A detailed description of the newly defined bio-oil yield and ER calculated considering the alcohol consumption is provided elsewhere [28].

$$\text{Yield of bio-oil (wt\%)} = \frac{\text{Mass of (dry ash free bio-oil + light fraction)}}{\text{Mass of (dry ash free biomass + solvent consumed)}} \times 100 \quad (7)$$

$$ER = \frac{(HHV_{oil} \times m_{oil}) + (HHV_{LF} \times \text{mass of LF})}{(HHV_{raw} \times m_{raw}) + (HHV_{sol} \times \text{mass of sol})} \times 100 \quad (8)$$

The HHV of the light fractions used for the calculation of ER is based on the average of HHVs of the ten most abundant chemical species in light bio-oil fraction analyzed via GC-TOF/MS both in case of scMeOH (Table S6) and scEtOH (Table S8), as discussed in a previous study [28]. Fig. 5 shows comparison of the bio-oil yields derived when ignoring and considering the alcohol consumption (Eqs. (1) and (7), respectively). When the alcohol consumption and the light fraction produced during the liquefaction are taken into account, a lower bio-oil yield results. More methanol is consumed (5.3 wt%) than ethanol (2.3 wt%), further indicating the higher reactivity of scMeOH, as discussed in Section 3.4.1. The yield of light fractions produced in scMeOH (20.5 wt%) is much higher than that in scEtOH (5.0 wt%). Thus, the increased consumption of methanol is the major reason for the decrease in the bio-oil yield from 66.0 wt% (Eq. (1)) to 51.1 wt% (Eq. (7)) for scMeOH liquefaction at 300 °C. Similarly, recalculation of the ER with considering the solvent consumption (Eq. (8)) decreases the ER of scMeOH liquefaction from 135 to 84%, and that of scEtOH liquefaction from 118 to 82%. Therefore, the yields of bio-oils produced from scMeOH and scEtOH as well as the ER values are similar when calculated considering the amount of solvent consumed during the liquefaction. Although more methanol is consumed and the recalculated values of the bio-oil yields and ER for scMeOH and scEtOH are similar, the low cost of methanol, which is approximately half that of ethanol [69], and the complete biomass conversion therein make methanol a more promising liquefaction solvent for carbohydrate-rich algal biomass.

Table 3
Chemical compositions of the liquid products collected as soon as the reactor was opened derived using GC-TOF/MS.

Compound types	scMeOH	scEtOH	subH$_2$O
	Area (%)		
Oxygen-containing species	81.5	81.6	33.9
Esters	54.6	47.2	–
Alcohols	11.2	4.0	4.0
Aromatics	1.0	1.0	0.1
Carboxylic acids	6.7	17.7	0.4
Ketones	2.7	2.6	22.7
Aldehydes	2.4	3.9	4.2
Heterocyclics	2.9	5.2	2.5
Nitrogen-containing species	13.8	15.2	33.8
Linear	3.8	4.5	2.4
Cyclics	6.1	9.4	28.5
Aromatics	3.9	1.3	3.0
Hydrocarbons	4.8	3.0	31.5
Linear	1.3	1.6	12.6
Cyclics	3.3	1.3	14.4
Aromatics	0.3	–	4.6
Methyl/methoxy-containing species	78.6	–	
Ethyl/ethoxy-containing species	–	58.2	

3.4.4. Bio-oil composition analysis

To understand the reactivity of alcohols in macroalgae liquefaction, GC-TOF/MS analyses were performed on the liquid products collected immediately after the reaction rather than on the dried bio-oil to characterize the light fractions that are typically lost during drying. The detected compounds (with area% > 0.1) are categorized into three major groups: oxygen-containing species, nitrogen-containing species, and hydrocarbons, as listed in Table 3. The details of the individual compounds and their classifications are listed in Tables S5, S7, and S9. Their representative GC-TOF/MS chromatograms are shown in Figs. S10, S11, and S12 for scMeOH, scEtOH, and subH$_2$O-based liquefactions, respectively. It is very difficult to draw any clear conclusions regarding the reaction mechanism based on the GC-TOF/MS results because of the complexity of the macroalgae and the liquid products. However, based on the categorization approach, some insight into the liquefaction behaviors of the three solvents could be obtained, as summarized below.

(1) In both the scMeOH and scEtOH cases, the oxygen-containing

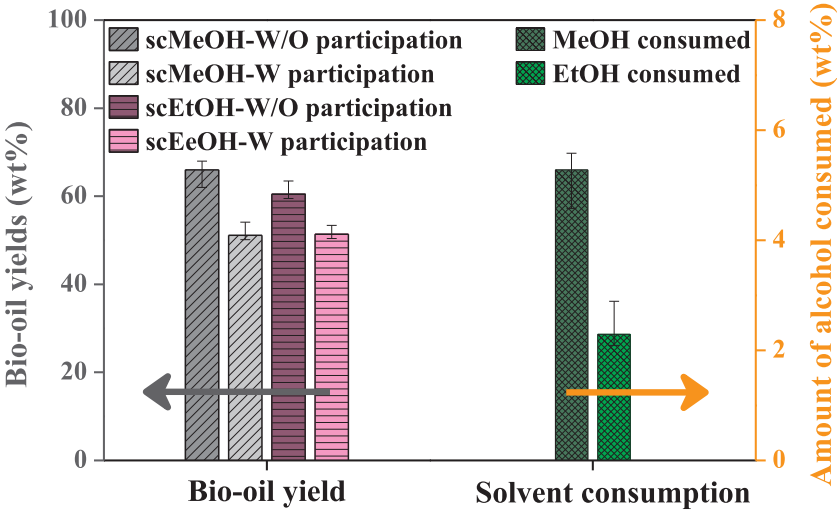

Fig. 5. Comparison of the alcohol consumption in the scMeOH and scEtOH liquefactions. Reaction conditions: 300 °C, 27.2 MPa (scMeOH), 21.9 MPa (scEtOH), 9.1 wt% for 30 min.

species present the highest area% followed by the nitrogen-containing species, and the hydrocarbons present the lowest area%. This is due to the composition of the macroalgae (51.0 wt% carbohydrates, 14.5 wt% of protein, Table 1). Conversely, in the subH_2O case, the area% of oxygen-containing, nitrogen-containing, and hydrocarbon species are quite similar. This may be caused by the selective extraction of hydrocarbon-rich species into the DCM/acetone phase during liquid-liquid separation. The major oxygen-containing species in the DCM/acetone phase are ketones (22.7 area%), which is a less polar species than carboxylic acids (0.4 area %) and alcohols (4.0 area%).

(2) Of the oxygen-containing species, esters present the highest area% in both the scMeOH and scEtOH cases, indicating that a high degree of esterification of carboxylic acids occurred. Carboxylic acids can be produced from carbohydrates by decomposition of monosaccharides [27,39] and from proteins by deamination of amino acids [22,39]. The higher area% of the esters resulting from the scMeOH-based liquefaction as compared to that for the scEtOH case is due to the higher esterification activity of scMeOH, as confirmed in previous studies [67,70]. This is also confirmed by the smaller area% of carboxylic acids observed in the scMeOH liquefaction (6.7 area%) as compared to that in the scEtOH liquefaction (17.7 area %).

(3) Both the scMeOH and scEtOH liquefactions present similar area% values for nitrogen-containing species (13.8 area% and 15.2 area%, respectively) and hydrocarbons (4.8 area% and 3.0 area%, respectively). Conversely, in the subH_2O liquefaction, the area% of nitrogen-containing species and hydrocarbons are much higher (33.8 area% and 31.5 area%) as compared to those of the alcohol liquefactions. This could be due to the selective partitioning of the less polar species to the DCM phase in the case of the subH_2O liquefaction.

(4) In order to infer the difference of reactivity of the two alcoholic solvents from the GC-TOF/MS results, the area% for the methyl/methoxy-containing compounds from the scMeOH liquefaction was compared with that of ethyl/ethoxy-containing compounds from the scEtOH liquefaction. The much higher area% of methyl/methoxy-containing compounds (78.6 area%) for the scMeOH-based liquefaction as compared to that of ethyl/ethoxy-containing compounds (58.2 area%) for the scEtOH-based liquefaction further confirms the higher reactivities of scMeOH toward alkylation and alkoxylation than those of scEtOH [68].

4. Conclusion

Herein, the potential of scMeOH in the liquefaction of carbohydrate-rich macroalgae (*Saccharina japonica*) was investigated. At the relatively low temperature of 300 °C, almost complete conversion of the macroalgae (98.1%) accompanied by a negligibly small amount of coke formation (1.9 wt%) and high bio-oil yield (66.0 wt%) was achieved. These values are higher than those for supercritical scEtOH liquefaction (87.8% conversion, 60.5 wt% bio-oil yield) and subH_2O liquefaction (91.9% conversion, 40.3 wt% bio-oil yield). In addition, the bio-oil produced in scMeOH exhibited a higher HHV (29.2 MJ kg^{-1}) and higher ER (135%) as compared to those produced in scEtOH (HHV = 27.8 MJ kg^{-1}; ER = 117.6%). Because of the greater reactivity of scMeOH, its consumption during the reaction is higher than that of scEtOH. However, the lower price of methanol and complete conversion makes scMeOH a highly promising candidate for carbohydrate-rich macroalgae liquefaction.

Acknowledgements

This study was supported by the New & Renewable Energy Core Technology Program (Grant Nos. 20143030090940 and 20143030100980) of the Korea Institute of Energy Technology Evaluation and Planning (KETEP) financed by the Ministry of Trade, Industry, and Energy of the Republic of Korea. The authors gratefully acknowledge additional support from Korea Electric Power Corporation through Korea Electrical Engineering & Science Research Institute (grant number: R15XA03-05).

Appendix A. Supplementary material

Supplementary data associated with this article can be found, in the online version, at http://dx.doi.org/10.1016/j.enconman.2017.08.092.

References

[1] Yu KL, Show PL, Ong HC, Ling TC, Chi-Wei Lan J, Chen W-H, et al. Microalgae from wastewater treatment to biochar – feedstock preparation and conversion technologies. Energy Convers Manage 2017;150:1–13.
[2] Chemodanov A, Jinjikhashvily G, Habiby O, Liberzon A, Israel A, Yakhini Z, et al. Net primary productivity, biofuel production and CO_2 emissions reduction potential of Ulva sp. (Chlorophyta) biomass in a coastal area of the Eastern Mediterranean. Energy Convers Manage 2017;148:1497–507.
[3] DEFRA. 2012 Guidelines to Defra/DECC's GHG conversion factors for company reporting; 2012.
[4] Chisti Y. Biodiesel from microalgae. Biotechnol Adv 2007;25:294–306.
[5] Zhou Y, Schideman L, Yu G, Zhang Y. A synergistic combination of algal wastewater treatment and hydrothermal biofuel production maximized by nutrient and carbon recycling. Energy Environ Sci 2013;6:3765.
[6] Ben Yahmed N, Jmel MA, Ben Alaya M, Bouallagui H, Marzouki MN, Smaali I. A biorefinery concept using the green macroalgae Chaetomorpha linum for the co-production of bioethanol and biogas. Energy Convers Manage 2016;119:257–65.
[7] Aitken D, Bulboa C, Godoy-Faundez A, Turrion-Gomez JL, Antizar-Ladislao B. Life cycle assessment of macroalgae cultivation and processing for biofuel production. J Clean Prod 2014;75:45–56.
[8] Mulligan CJ, Strezov L, Strezov V. Thermal decomposition of wheat straw and mallee residue under pyrolysis conditions. Energy Fuels 2010;24:46–52.
[9] Hossain MK, Strezov V, Nelson PF. Thermal characterisation of the products of wastewater sludge pyrolysis. J Anal Appl Pyrolysis 2009;85:442–6.
[10] Kim SS, Ly HV, Choi GH, Kim J, Woo HC. Pyrolysis characteristics and kinetics of the alga Saccharina japonica. Biores Technol 2012;123:445–51.
[11] Yu G, Zhang Y, Schideman L, Funk T, Wang Z. Distributions of carbon and nitrogen in the products from hydrothermal liquefaction of low-lipid microalgae. Energy Environ Sci 2011;4:4587.
[12] Brown TM, Duan P, Savage PE. Hydrothermal liquefaction and gasification of Nannochloropsis sp. Energy Fuels 2010;24:3639–46.
[13] Jena U, Das KC, Kastner JR. Effect of operating conditions of thermochemical liquefaction on biocrude production from Spirulina platensis. Biores Technol 2011;102:6221–9.
[14] Vardon DR, Sharma BK, Scott J, Yu G, Wang Z, Schideman L, et al. Chemical properties of biocrude oil from the hydrothermal liquefaction of Spirulina algae, swine manure, and digested anaerobic sludge. Biores Technol 2011;102:8295–303.
[15] Garcia Alba L, Torri C, Samorì C, van der Spek J, Fabbri D, Kersten SRA, et al. Hydrothermal treatment (HTT) of microalgae: evaluation of the process as conversion method in an algae biorefinery concept. Energy Fuels 2012;26:642–57.
[16] Yang W, Li X, Liu S, Feng L. Direct hydrothermal liquefaction of undried macroalgae Enteromorpha prolifera using acid catalysts. Energy Convers Manage 2014;87:938–45.
[17] Elliott DC. Review of recent reports on process technology for thermochemical conversion of whole algae to liquid fuels. Algal Res 2016;13:255–63.
[18] Anastasakis K, Ross AB. Hydrothermal liquefaction of the brown macro-alga Laminaria saccharina: effect of reaction conditions on product distribution and composition. Biores Technol 2011;102:4876–83.
[19] Brand S, Susanti RF, Kim SK, Lee H-s, Kim J, Sang B-I. Supercritical ethanol as an enhanced medium for lignocellulosic biomass liquefaction: influence of physical process parameters. Energy 2013;59:173–82.
[20] Zhou D, Zhang L, Zhang S, Fu H, Chen J. Hydrothermal liquefaction of macroalgae Enteromorpha prolifera to bio-oil. Energy Fuels 2010;24:4054–61.
[21] Aysu T, Küçük MM, Demirbaş A. Optimization of process variables for supercritical liquefaction of giant fennel. RSC Adv 2014;4:55912–23.
[22] Yuan X, Wang J, Zeng G, Huang H, Pei X, Li H, et al. Comparative studies of thermochemical liquefaction characteristics of microalgae using different organic solvents. Energy 2011;36:6406–12.
[23] Duan P, Jin B, Xu Y, Yang Y, Bai X, Wang F, et al. Thermo-chemical conversion of Chlorella pyrenoidosa to liquid biofuels. Biores Technol 2013;133:197–205.
[24] Chen Y, Wu Y, Hua D, Li C, Harold MP, Wang J, et al. Thermochemical conversion of low-lipid microalgae for the production of liquid fuels: challenges and opportunities. RSC Adv 2015;5:18673–701.
[25] Brand S, Hardi F, Kim J, Suh DJ. Effect of heating rate on biomass liquefaction: differences between subcritical water and supercritical ethanol. Energy 2014;68:420–7.
[26] Brand S, Kim J. Liquefaction of major lignocellulosic biomass constituents in supercritical ethanol. Energy 2015;80:64–74.
[27] Zhou D, Zhang S, Fu H, Chen J. Liquefaction of macroalgae Enteromorpha prolifera in sub-/supercritical alcohols: direct production of ester compounds. Energy Fuels

2012;26:2342–51.
[28] Zeb H, Choi J, Kim Y, Kim J. A new role of supercritical ethanol in macroalgae liquefaction (Saccharina japonica): understanding ethanol participation, yield, and energy efficiency. Energy 2017;118:116–26.
[29] Miller GL, Miller EE. Determination of nitrogen in biological materials. Anal Chem 1948;20:481–8.
[30] Folch J, Lees M, Stanley SGH. A simple method for the isolation and purification of total lipids from animal tissues. J Biol Chem 1957;226:497–509.
[31] Van den Bosch S, Schutyser W, Vanholme R, Driessen T, Koelewijn SF, Renders T, et al. Reductive lignocellulose fractionation into soluble lignin-derived phenolic monomers and dimers and processable carbohydrate pulps. Energy Environ Sci 2015;8:1748–63.
[32] Zeb H, Riaz A, Kim J. Understanding the effect of biomass-to-solvent ratio on macroalgae (Saccharina japonica) liquefaction in supercritical ethanol. J Supercrit Fluids 2017;120:65–74.
[33] Susanti RF, Dianningrum LW, Yum T, Kim Y, Lee BG, Kim J. High-yield hydrogen production from glucose by supercritical water gasification without added catalyst. Int J Hydrogen Energy 2012;37:11677–90.
[34] López Barreiro D, Prins W, Ronsse F, Brilman W. Hydrothermal liquefaction (HTL) of microalgae for biofuel production: state of the art review and future prospects. Biomass Bioenerg 2013;53:113–27.
[35] Tian C, Li B, Liu Z, Zhang Y, Lu H. Hydrothermal liquefaction for algal biorefinery: a critical review. Renew Sustain Energy Rev 2014;38:933–50.
[36] Chow MC, Jackson WR, Chaffee AL, Marshall M. Thermal treatment of algae for production of biofuel. Energy Fuels 2013;27:1926–50.
[37] Levine RB, Pinnarat T, Savage PE. Biodiesel production from wet algal biomass through in situ lipid hydrolysis and supercritical transesterification. Energy Fuels 2010;24:5235–43.
[38] Chen Y, Wu Y, Zhang P, Hua D, Yang M, Li C, et al. Direct liquefaction of Dunaliella tertiolecta for bio-oil in sub/supercritical ethanol-water. Biores Technol 2012;124:190–8.
[39] Zhang J, Chen WT, Zhang P, Luo Z, Zhang Y. Hydrothermal liquefaction of Chlorella pyrenoidosa in sub- and supercritical ethanol with heterogeneous catalysts. Biores Technol 2013;133:389–97.
[40] Zhang J, Zhang Y. Hydrothermal liquefaction of microalgae in an ethanol–water co-solvent to produce biocrude oil. Energy Fuels 2014;28:5178–83.
[41] Huang H, Yuan X, Zeng G, Wang J, Li H, Zhou C, et al. Thermochemical liquefaction characteristics of microalgae in sub- and supercritical ethanol. Fuel Process Technol 2011;92:147–53.
[42] Singh R, Bhaskar T, Balagurumurthy B. Effect of solvent on the hydrothermal liquefaction of macro algae Ulva fasciata. Process Saf Environ Prot 2015;93:154–60.
[43] Neveux N, Yuen AK, Jazrawi C, Magnusson M, Haynes BS, Masters AF, et al. Biocrude yield and productivity from the hydrothermal liquefaction of marine and freshwater green macroalgae. Biores Technol 2014;155:334–41.
[44] Schumacher M, Yanık J, Sınağ A, Kruse A. Hydrothermal conversion of seaweeds in a batch autoclave. J Supercrit Fluids 2011;58:131–5.
[45] Bae YJ, Ryu C, Jeon JK, Park J, Suh DJ, Suh YW, et al. The characteristics of bio-oil produced from the pyrolysis of three marine macroalgae. Biores Technol 2011;102:3512–20.
[46] Li J, Wang G, Wang Z, Zhang L, Wang C, Yang Z. Conversion of Enteromorpha prolifera to high-quality liquid oil via deoxy-liquefaction. J Anal Appl Pyrolysis 2013;104:494–501.
[47] Singh R, Balagurumurthy B, Bhaskar T. Hydrothermal liquefaction of macro algae: effect of feedstock composition. Fuel 2015;146:69–74.
[48] Leow S, Witter JR, Vardon DR, Sharma BK, Guest JS, Strathmann TJ. Prediction of microalgae hydrothermal liquefaction products from feedstock biochemical composition. Green Chem 2015;17:3584–99.
[49] Valdez PJ, Nelson MC, Wang HY, Lin XN, Savage PE. Hydrothermal liquefaction of Nannochloropsis sp.: systematic study of process variables and analysis of the product fractions. Biomass Bioenerg 2012;46:317–31.
[50] Li D, Chen L, Xu D, Zhang X, Ye N, Chen F, et al. Preparation and characteristics of bio-oil from the marine brown alga Sargassum patens C. Agardh. Bioresour Technol 2012;104:737–42.
[51] Jin B, Duan P, Xu Y, Wang F, Fan Y. Co-liquefaction of micro- and macroalgae in subcritical water. Biores Technol 2013;149:103–10.
[52] Zou S, Wu Y, Yang M, Li C, Tong J. Bio-oil production from sub- and supercritical water liquefaction of microalgae Dunaliella tertiolecta and related properties. Energy Environ Sci 2010;3:1073–8.
[53] Guo Y, Yeh T, Song W, Xu D, Wang S. A review of bio-oil production from hydrothermal liquefaction of algae. Renew Sustain Energy Rev 2015;48:776–90.
[54] Yan Y, Xu J, Li T, Ren Z. Liquefaction of sawdust for liquid fuel. Fuel Process Technol 1999;60:135–43.
[55] Xu C, Etcheverry T. Hydro-liquefaction of woody biomass in sub- and super-critical ethanol with iron-based catalysts. Fuel 2008;87:335–45.
[56] Chumpoo J, Prasassarakich P. Bio-oil from hydro-liquefaction of bagasse in supercritical ethanol. Energy Fuels 2010;24:2071–7.
[57] Hidajat MJ, Riaz A, Park J, Insyani R, Verma D, Kim J. Depolymerization of concentrated sulfuric acid hydrolysis lignin to high-yield aromatic monomers in basic sub- and supercritical fluids. Chem Eng J 2017;317:9–19.
[58] Liu Z, Zhang F-S. Effects of various solvents on the liquefaction of biomass to produce fuels and chemical feedstocks. Energy Convers Manage 2008;49:3498–504.
[59] Cortesia C, Vilcheze C, Bernut A, Contreras W, Gomez K, de Waard J, et al. Acetic acid, the active component of vinegar, is an effective tuberculocidal disinfectant. MBio 2014;5:e00013–4.
[60] Zhang S, Duan X, Ye L, Lin H, Xie Z, Yuan Y. Production of ethanol by gas phase hydrogenation of acetic acid over carbon nanotube-supported Pt–Sn nanoparticles. Catal Today 2013;215:260–6.
[61] Jones B, Linnen M, Tande B, Seames W. The production of vinyl acetate monomer as a co-product from the non-catalytic cracking of soybean oil. Processes 2015;3:619–33.
[62] Castillo Martinez FA, Balciunas EM, Salgado JM, Domínguez González JM, Converti A. Oliveira RPdS. Lactic acid properties, applications and production: a review. Trends Food Sci Technol 2013;30:70–83.
[63] Baumann I, Westermann P. Microbial production of short chain fatty acids from lignocellulosic biomass: current processes and market. Biomed Res Int 2016;2016:15.
[64] Long J, Xu Y, Wang T, Yuan Z, Shu R, Zhang Q, et al. Efficient base-catalyzed decomposition and in situ hydrogenolysis process for lignin depolymerization and char elimination. Appl Energy 2015;141:70–9.
[65] McIver J, Robert T, Scott JA, Riveros JM. Effect of solvation on the intrinsic relative acidity. J Am Chem Soc 1973;95:2706–8.
[66] Cinlar B, Wang T, Shanks BH. Kinetics of monosaccharide conversion in the presence of homogeneous Bronsted acids. Appl Catal A 2013;450:237–42.
[67] Warabi Y, Kusdiana D, Saka S. Reactivity of triglycerides and fatty acids of rapeseed oil in supercritical alcohols. Biores Technol 2004;91:283–7.
[68] Horikawa Y, Uchino Y, Sako T. Alkylation and acetal formation using supercritical alcohol without catalyst. Chem Lett 2003;32:232–3.
[69] Tarud J, Phillips S. Technoeconomic comparison of biofuels: ethanol, methanol, and gasoline from gasification of woody residues. Am Chem Soc Nat Meeting. 2011. NREL/PR-5100-52636.
[70] Demirbas A. Production of biodiesel fuels from linseed oil using methanol and ethanol in non-catalytic SCF conditions. Biomass Bioenerg 2009;33:113–8.